ON FREQUENCY LOCK DETECTION FOR LOW SIGNAL-TO-NOISE RATIO (SNR) QAM SIGNALS

Doan Nguyen Vo and Steve Ricard
Ultra Electronics TCS Inc., Montreal, Quebec, Canada,
{doan-nguyen.vo, steve.ricard}@ultra-tcs.com

ABSTRACT

This work proposes a new approach on the frequency lock detection suitable for high QAM modulations which are used in many reconfigurable Software-Defined-Radio (SDR) systems. This work contains a reliable mechanism to enable a radio system working under very low signal-to-noise ratio (SNR) environments, with high coding gain scenarios such as TPC, LDPC, etc.

1. INTRODUCTION

In a common SDR receiver, the modulated signal after being processed by the analog front-end (AFE) is sampled and converted into digital signal. The received signal is further processed by using digital signal processing (DSP) techniques. One of the receiver's key functions is to extract the correct carrier frequency so that a complete baseband signal could be recovered.

In summary, the modem is first reset when powered up. The carrier recovery (CR) control block is in the state to initialize all parameters required by CR loop's blocks. The CR is claimed "locked" when it detects that its internal requirements exceed PASS thresholds, and the modem backend declares its frame detection being passed. In the "locked" state, the modem performs "tracking" of the parameters (frequency, phase, timing, etc.). For some unforeseen problems such as fades, jams, etc., the modem gets "unlock" state. Prior to "locked", fast operations are performed to acquire information for the parameters.

In some military communication systems, we frequently encounter critical problems: (1) the system must be robust against high noise, and (2) the data stream contains no known pattern (i.e. preamble for data training is prohibited) because it is susceptive to enemies' listening and/or jamming. In addition, specifications of fast acquisition and re-acquisition would require highly reliable and robust techniques for synchronizations.

We propose special lock detection for the frequency offset based on CFAR (Constant False Alarm Rate). In some previous applications [5], the technique is based on the correlation properties between the received symbols and the corresponding expected ones (training sequence). The technique was used mainly for BPSK, and the training sequence is carefully selected in order to maximize the gap in probability of lock and unlock.

$$F = \frac{\left(\sum_{k=1}^{N} a_I(k) z_I(k)\right)^2 + \left(\sum_{k=1}^{N} a_Q(k) z_Q(k)\right)^2}{\sum_{k=1}^{N} \|z(k)\|^2} > \alpha \qquad (1)$$

We adopt this algorithm for high QAM with some modifications. The correlation between the received symbols and the detected symbols is considered. The metric is normalized with the power of the symbols. Since the energy of the symbols is unchanged, the metric is maximized when the symbols are in their expected regions, i.e., offset frequency and phase are 0. The metric F is compared with a threshold □ to decide whether it is locked.

The metric F is only a representative notation to ease the mathematical analysis. In real implementation, the numerator of F will be compared with the denominator of F multiplying with the threshold. This avoids the division operation in the proposed metric.

The structure of the paper is as follows. Section II presents the proposed technique. Section III shows analytical bounds of the lock and unlocked metrics for different QAMs. Simulation graphs with Matlab are included to depict the analytical values for different Eb/No and frequency offset.

2. THE PROPOSED LOCK METRIC

There are two problems when the above technique is directly applied for high QAMs. First the sequence a(k) is no longer known, but random. Secondly the correlation values become even weaker for higher QAMs. These problems result a small difference between lock and unlock metric to distinguish. That means the probability of false alarm of the detection is high;

i.e., the detection is not reliable. We modify the technique so that it could be used for high QAM applications. The idea is to consider the diagonal points to provide a better correlation property. This section shows how to select a good combination of constellation points in other to improve the gap between lock and unlock metric.

2.1. For Square QAMs (4, 16, and 64)

In section, the square QAMs such as QAM-4, 16, and 64 are considered. A normalized metric function for *M*-QAM is proposed as,

$$F_{squareQAM} = \sqrt{M}\frac{\left(\sum_{k=1}^{N} a_I(k)z_I(k)\right)^2 + \left(\sum_{k=1}^{N} a_Q(k)z_Q(k)\right)^2}{\sum_{k=1}^{N}\|a(k)\|^2 \sum_{k=1}^{N}\|z(k)\|^2} > \alpha \qquad (2)$$

In this function, $z(k)$ is a received noisy symbol, $a(k)$ is its corresponding hard-decision symbol, M is the QAM order, and N is the total number of symbols to be considered. The scaling factor is added so that the metric F will be at 1 when locked at high SNR.

An example for QAM-16 is shown as below. In this example, only diagonal points (blue regions or $|a_I| = |a_Q|$,) are considered. Points not on the diagonals will be forced to have $a(k)=0$.

The technique considers the constellation points not on the diagonal axes as noise adding up to the energy portion of the metric. It does not impact much when it is locked, but it helps when it is unlock. When it is unlock, the diagonal points will be rotated and it has less percentage of staying in the right location; other rotating points can get into the diagonal axes, but has less probability compared with the probability of the good diagonal points rotating out their location. It will provide (1) the average power of the measured diagonal points is reduced, and (2) the energy of noise-like power is increased. These impacts will make the metric significantly smaller compared with the metric when locked.

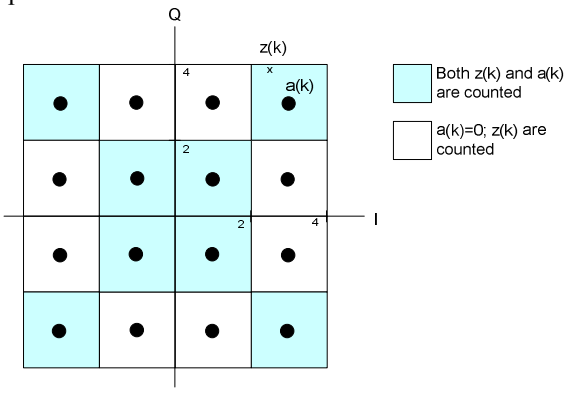

Figure 1 - Example of selection of constellation points for QAM-16

2.2. For Cross QAMs (32 and 128)

The above proposed metric function can work with square QAMs where the average energy of the diagonal points is equal to the average of the total constellation points. For cross QAMs (i.e., 32 or 128), this nice property is not applicable. Another approach will be proposed.

The new metric function is slightly modified as,

$$F_{crossQAM} = 2\frac{\left(\sum_{k=1}^{N} a_I(k)z_I(k)\right)^2 + \left(\sum_{k=1}^{N} a_Q(k)z_Q(k)\right)^2}{\sum_{k=1}^{N}\|a(k)\|^2 \sum_{k=1}^{N}\|z(k)\|^2} > \alpha \qquad (3)$$

In this function, the definitions of $z(k)$, $a(k)$, and N are as the same as in the previous section. The scaling factor is added so that the metric F will be at 1 when locked at high SNR.

An example for QAM-32 is shown as below. The difference in this case is that only diagonal points (i.e., $|a_I| = |a_Q|$) will be considered. The points in the blue regions are counted towards the metric. The points at the 4 corners (red regions) will have their detected symbol value $a(k)=0$. The other points (in white regions) not on these axes will be ignored in all computations.

Intuitively the points at the corners help to reduce the metric when the system is unlocked. These points are considered as noise-like power as in the previous case. The power at these corners is significantly large and it can be seen as a weighting factor. We currently use the actual measured energy, but it can be replaced by a predefined average energy.

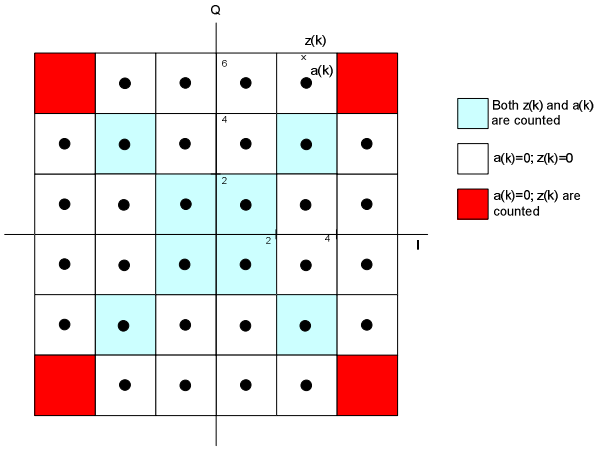

Figure 2 - Example of Constellation points for QAM-32

3. MATHMATICAL PROPERTIES

This section derives the mathematical properties of the metric function.

3.1. Behavior with noise

It is noticed that the numerator part of the proposed metrics for both square and cross QAMs is actually a correlator. The summations in the correlator would neutralize the effect of noise, assuming that noise is white Gaussian distributed and both data and noise are statistically independent. Thus the numerator would not vary much with noise. The denominator is, in the other hand, growing with noise as $E\left(\|z(k)\|^2\right) \cong E\left(\|a(k)\|^2 + \|n(k)\|^2\right)$.

This proves that the metric decreases as noise increases compared with the signal.

This property is important, because in order to have a reliable indication when locked or unlocked, the metric must be controlled such as

$$F_{lock,\min} \geq \alpha > F_{unlock,\max} \tag{4}$$

The above property suggests that $F_{lock,\ \min}$=$F_{lock,\text{minSNR}}$ and $F_{unlock,\ \max}$=$F_{unlock,\text{no noise}}$.

It is therefore sufficient to study the metric (1) at locked state at low SNR, and (2) unlocked state at no noise, as in the following sections.

3.2. An Approximation of the Detector Metric at Locked State

It is possible to obtain the values of the detector when it is in lock. The assumption of only AWGN contributions is valid at the output of the equalizer when the channel effects are eliminated or minimized. We show different computations for two different cases of QAMs as below.

3.2.1. Square QAMs (4, 16 and 64)

For square QAMs, the diagonal points have the average energy equal to the average E_s of the whole constellation.

$$E[a_{diag}^2(k)] = \frac{1}{N}\sum_{n=1}^{N} 2(2n-1)^2 = \frac{8N^2-2}{3} = E_s \tag{5}$$

$$E[a_{I,diag}^2(k)] = E[a_{Q,diag}^2(k)] = E[a_{diag}^2(k)]/2 = E_s/2 \tag{6}$$

In M constellation points of the squared QAM, the total number of diagonal points is $2\sqrt{M}$. Therefore, in average, for N observation points, there would have $2N/\sqrt{M}$ diagonal points, assuming that the data is random and statistically independent. Therefore, on locked, it can be shown that the metric function in Eq. 2 converges to,

$$F_{lock} \cong \sqrt{M}\,\frac{2\left(\frac{2N}{\sqrt{M}}\right)^2\frac{E_s^2}{4}}{\frac{2N}{\sqrt{M}}E_s\cdot N\left(E_s+\sigma_n^2\right)} = \frac{1}{1+\frac{\sigma_n^2}{E_s}} \tag{7}$$

$$F_{lock} = \frac{1}{1+1/SNR} \xrightarrow{SNR>>1} 1 \tag{8}$$

The equations depicts that the metric is inversely proportional with noise. However, high QAMs (such as 16-QAM or 64-QAM), the operating SNR (for raw BER~1E-2) is much larger than 1, thus Eq. 8 shows that it would be around 1. The simulations are shown in Appendix. These results indicate the above approximations are accurate.

3.2.2. Cross QAMs (32 and 128)

For cross QAMs, the metric function when locked can be approximated as

$$F_{lock} \cong \frac{1}{1+1/SNR}\left(\frac{1}{1+4Q\left(\sqrt{\frac{3SNR}{M-1}}\right)}\right) \xrightarrow{SNR>>1} 1 \tag{9}$$

The simulations are shown in Appendix. These simulation results indicate the above approximation is fairly accurate.

3.3. Bounds of the Detector Metric at Unlocked State

The exact expression of the metric when unlock is complex; we are indeed interested in their bound. We observe that the diagonal points are in fact a collection of many QAM-4 constellations at different amplitudes. We will show that the two metric functions of square and cross QAMs are bounded under the same metric of these diagonal points.

The metric for square QAMs can be rewritten as follows,

$$\begin{aligned} F_{unlock,squareQAM} &= \sqrt{M}\,\frac{\left(\sum_{k=1}^{N} a_I(k)z_I(k)\right)^2 + \left(\sum_{k=1}^{N} a_Q(k)z_Q(k)\right)^2}{\sum_{k=1}^{N}\|a(k)\|^2\sum_{k=1}^{N}\|z(k)\|^2} \\ &= \sqrt{M}\,\frac{\left(\sum_{k=1}^{L} a_I(k)z_I(k)\right)^2 + \left(\sum_{k=1}^{L} a_Q(k)z_Q(k)\right)^2}{\sum_{k=1}^{L}\|a(k)\|^2\sum_{k=1}^{N}\|z(k)\|^2} \end{aligned} \tag{10}$$

where L is number of the diagonal points. We note that when it is unlock, the constellation is rotating and the percentage of points fall in the diagonal axes drops significantly. That means the average power of the diagonal points will be reduced, i.e.,

$$\sum_{k=1}^{N}\|z(k)\|^2 \geq \sum_{k=1}^{N}\|a(k)\|^2 = \frac{N}{L}\sum_{k=1}^{L}\|a(k)\|^2 = \frac{\sqrt{M}}{2}\sum_{k=1}^{L}\|a(k)\|^2 \tag{11}$$

It can be shown that

$$\begin{aligned} F_{unlock,squareQAM} &< \sqrt{M}\,\frac{\left(\sum_{k=1}^{N} a_I(k)z_I(k)\right)^2 + \left(\sum_{k=1}^{N} a_Q(k)z_Q(k)\right)^2}{\sum_{k=1}^{N}\|a(k)\|^2\sum_{k=1}^{L}\|a(k)\|^2\frac{\sqrt{M}}{2}} \\ &= 2\,\frac{\left(\sum_{k=1}^{L} a_I(k)z_I(k)\right)^2 + \left(\sum_{k=1}^{L} a_Q(k)z_Q(k)\right)^2}{\left(\sum_{k=1}^{L}\|a(k)\|^2\right)^2} = F_{unlock,crossQAM} \end{aligned} \tag{12}$$

That depicts the performances of square QAMs are better than the one of cross QAMs.

Replace the summation notation with the average, the metric will become

$$F_{unlock} < 2\frac{\left(NE\left[a_I(k)z_I(k)\right]\right)^2 + \left(NE\left[a_Q(k)z_Q(k)\right]\right)^2}{\left(NE_s\right)^2} = 2\frac{\left(E\left[a_I(k)z_I(k)\right]\right)^2 + \left(E\left[a_Q(k)z_Q(k)\right]\right)^2}{E_s^2} \quad (13)$$

Note that when unlock, the received symbol is rotated with an angle θ.

$$z(k) = a(k)e^{j\theta} = a_I\cos\theta_k - a_Q\sin\theta_k + j(a_I\sin\theta_k + a_Q\cos\theta_k)$$

$$E\left[a_I(k)z_I(k)\right] = E\left[a_I(k)z_I(k)\right] = E\left[a_I^2\cos\theta_k - a_Ia_Q\sin\theta_k\right]$$

$$= \frac{E_s}{2}E[\cos\theta_k] = \frac{E_s}{2}\frac{2}{\pi}\int_{-\pi/4}^{\pi/4}\cos\theta d\theta = \frac{E_s}{2}\frac{2\sqrt{2}}{\pi}$$

Thus the metric for QAMs is bound at,

$$F_{unlock,QAM} < 2\frac{2\left(\frac{E_s}{2}\frac{2\sqrt{2}}{\pi}\right)^2}{E_s^2} = \frac{8}{\pi^2} \cong 0.81 \quad (14)$$

We performed some simulations to verify the behaviors of the QAM modulations when the system is under unlock. The results are included in Appendix.

4. IMPLEMENTATION

The realization of the lock metric could be easily obtained as shown in Figure 5. The block diagram shows how the overall lock metric is implemented, with details in quantization and pipelines. The implementation works well in FPGAs. As shown in the block diagram, the input values were 16 bits in the sample design. There was a digital AGC in the sample design and the metric computation was done accordingly. The slicing function is a very simple hard-decision circuit. The target FPGA device was an Altera Stratix-3 with industrial grade (EP3SE110F780I4). The circuit computes the metric over a programmable range of symbol. It is noticed that the observation window *NN* is a power of 2 to ease the computation and obtain a simpler design. The Altera device was compiled with the metric circuit only using Quartus 9.1 software. The resource usage was 1250 ALUTs, 605 flip-flops and 20 DSP blocks. The maximum clock frequency was close to 300MHz and the symbol rate was up to 60Msymbols/s. Further hardware optimization could be obtained if resource reuse is applied.

5. CONCLUSION

The work presented in this paper covers mathematical proof of the frequency lock detection process, its simulations, and the implementation on FPGA. The results are promising to enable reliable detections at low SNR, suitable for applications with strong coding such as TPC, LDPC.

ACKNOWLEDGMENT

We would like to express our most sincere gratitude to Ultra Electronics TCS for supporting us during this project. Special thanks to Mr. Michel Forté for his enthusiasm to revise the mathematical equations and opinion sharing.

REFERENCES

[1] U. Mengali and A. N. D'Andrea, *Synchronization Techniques for Digital Receivers*, Plenum Press, 1997.

[2] N. D. Vo and T. Le-Ngoc, "Maximum Likelihood (ML) Symbol Timing Recovery (STR) Techniques for Reconfigurable PAM and QAM Modems," *International Jounal of Wireless Personal Communications*, Springer, Netherlands, vol. 41, no. 3, May, 2007, pp. 379-391.

[3] Fu WenJun et al., "Design and Performance Evaluation of Carrier Lock Detection in Digital QPSK Receiver," *2006 IEEE International Conference on Communications*, vol. 7, June 2006, pp. 2941 – 2945.

[4] Kyung Ha Lee et al., "A novel digital lock detector for QPSK receiver," *IEEE Transactions on Communications*, vol. 46, issue 6, June 1998, pp. 750 – 753.

[5] M.R. Soleymani and H. Girard, "The effect of the frequency offset on the probability of miss in a packet modem using CFAR detection method," *IEEE Transactions on Communications*, vol. 40, iss. 7, July 1992, pp. 1205 – 1211.

APPENDIX

A.1. Simulated metric when locked

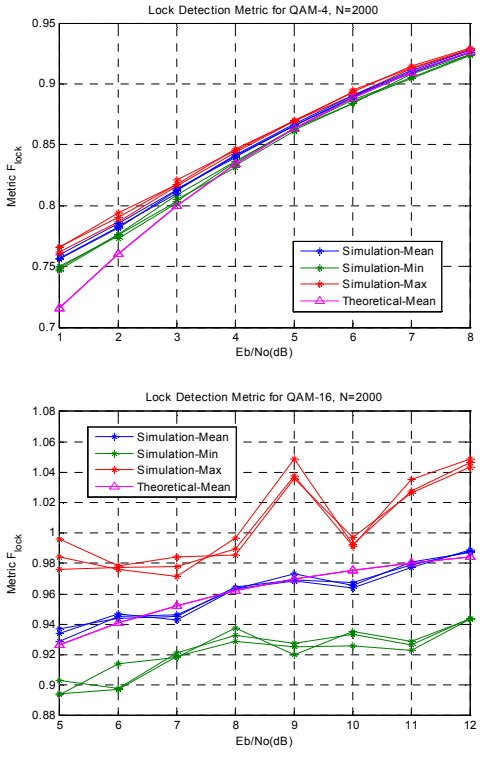

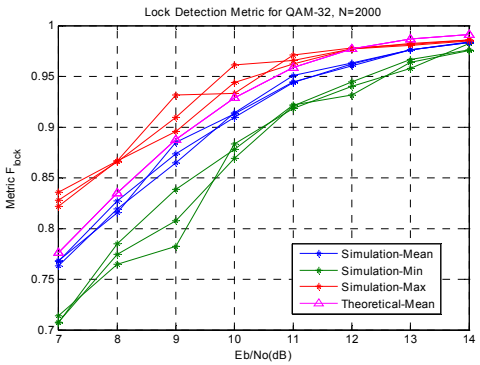

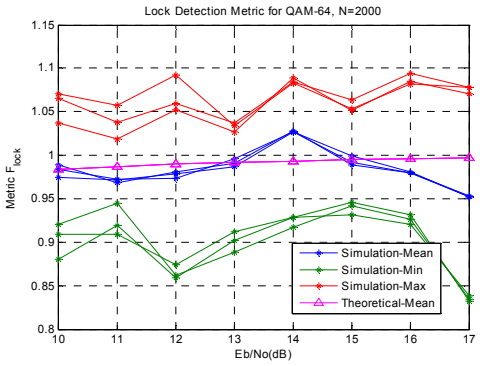

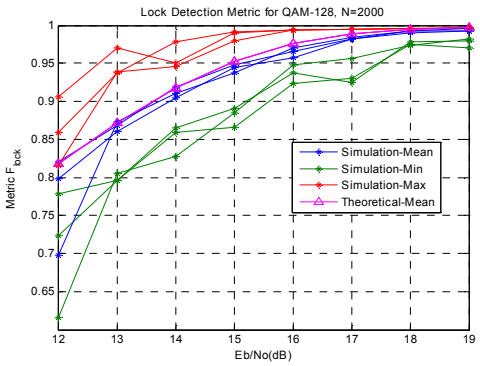

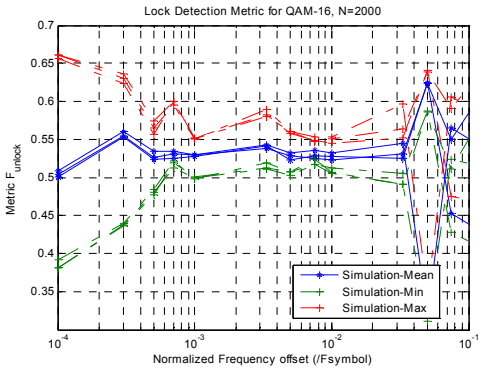

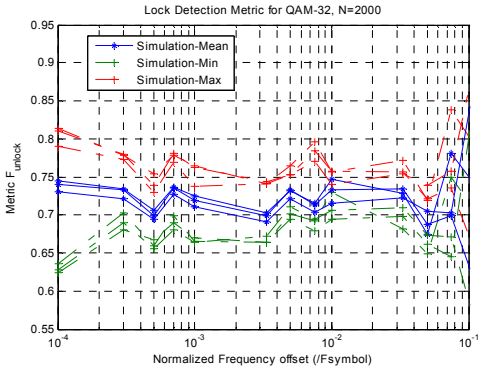

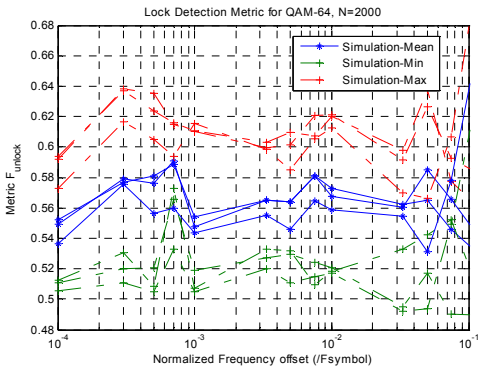

Figure 3 – Lock metric values when locked vs. E_b/N_o for different QAMs

A.2. Simulated metric when unlocked

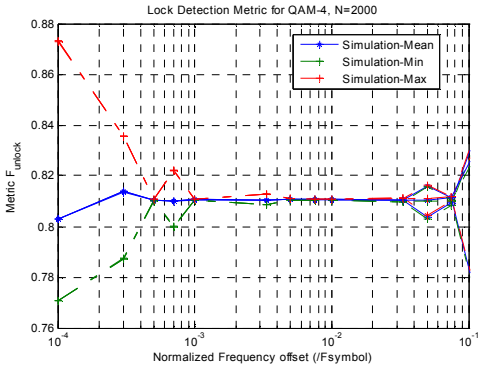

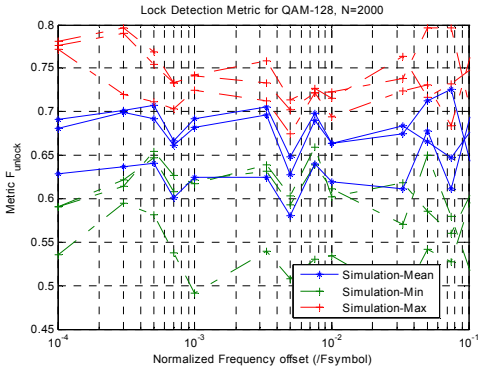

Figure 4 – Metric values when unlocked for different QAMs.

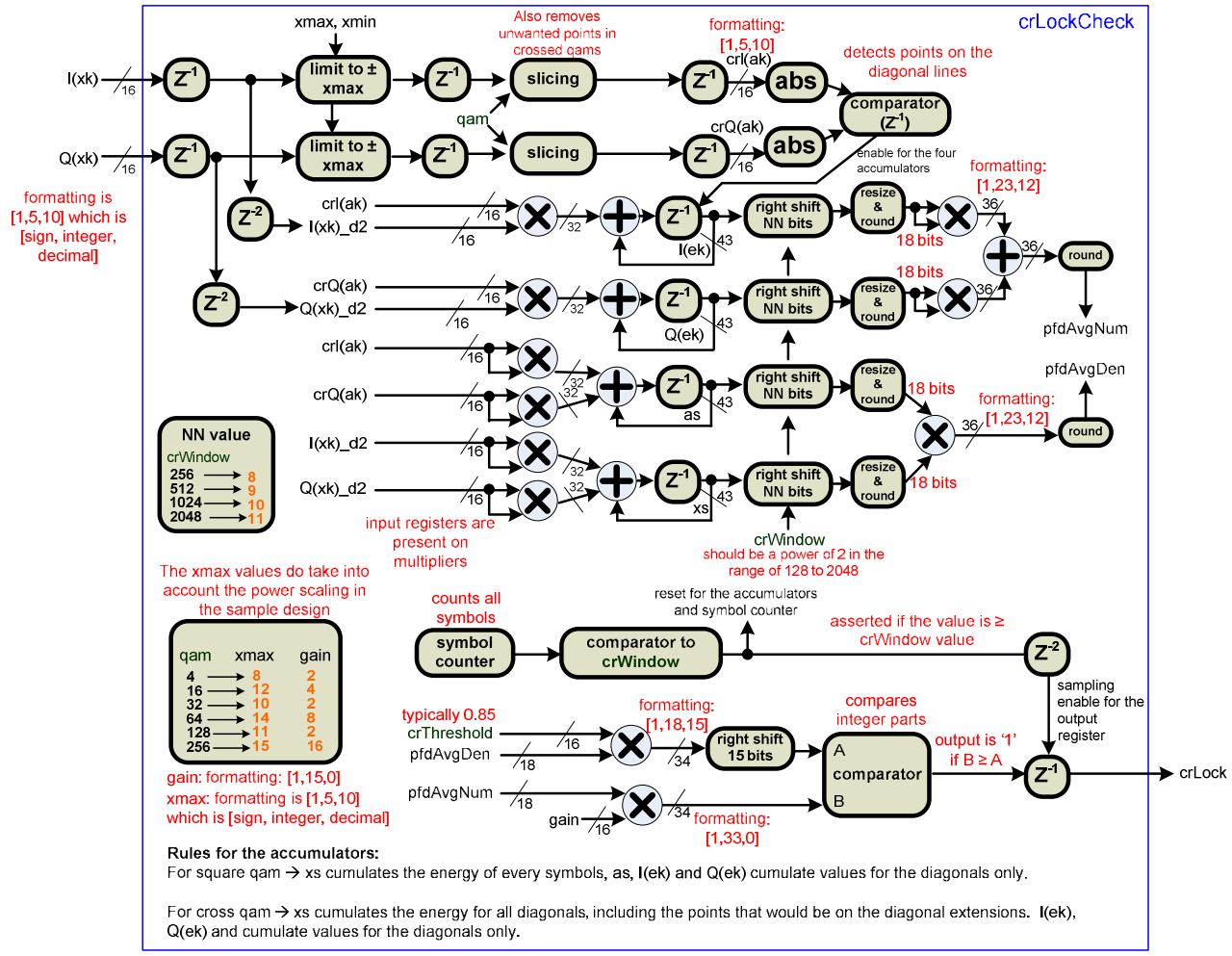

Figure 5 - Implementation of the metric in FPGA

Copyright Transfer Agreement: The following Copyright Transfer Agreement must be included on the cover sheet for the paper (either email or fax)—not on the paper itself.

"The authors represent that the work is original and they are the author or authors of the work, except for material quoted and referenced as text passages. Authors acknowledge that they are willing to transfer the copyright of the abstract and the completed paper to the SDR Forum for purposes of publication in the SDR Forum Conference Proceedings, on associated CD ROMS, on SDR Forum Web pages, and compilations and derivative works related to this conference, should the paper be accepted for the conference. Authors are permitted to reproduce their work, and to reuse material in whole or in part from their work; for derivative works, however, such authors may not grant third party requests for reprints or republishing."

Government employees whose work is not subject to copyright should so certify. For work performed under a U.S. Government contract, the U.S. Government has royalty-free permission to reproduce the author's work for official U.S. Government purposes.